Journal of Magnetic Resonance **137,** 231–236 (1999)
Article ID jmre.1998.1690, available online at http://www.idealibrary.com on IDEAL®

Velocity Selective Radiofrequency Pulse Trains

David G. Norris[1] and Christian Schwarzbauer

Max-Planck-Institute of Cognitive Neuroscience, Stephanstrasse 1a, 04103 Leipzig, Germany

Received September 2, 1998; revised December 1, 1998

The incorporation of velocity-encoding gradient pulses in RF-pulse trains is proposed and examined. Velocity selective perturbation is shown to be analogous in many respects to the well established use of trains of short RF-pulses for chemical shift selective perturbation. Velocity selective perturbation is viable in a biomedical setting only if additional RF refocusing pulses are inserted between the individual RF-pulse elements. Aspects of velocity selective excitation saturation and inversion are examined, and new inversion pulse trains proposed. The selective perturbation of both flowing and stationary spins is demonstrated in phantoms and possible biomedical applications of these pulse trains are discussed. © 1999 Academic Press

Key Words: **velocity selective perturbation; RF-pulse.**

INTRODUCTION

Trains of short RF-pulses (*1, 2*) are an established method for achieving solvent suppression in NMR spectroscopy (*3*). The principle of operation of these pulse trains is that the evolution of the chemical shift between the individual RF-pulse elements modulates the pulse angle. The pulse angle as a function of chemical shift is determined by the phase of the magnetization at the time of the RF-pulse elements, and not by its value at intermediate times. The earliest, and still commonly used, pulse trains of this type had intensities determined according to binomial coefficients (*2*). It has long been established (*4–6*) that position, and its time derivatives, can be phase-encoded by means of pulsed magnetic field gradients, and particularly that velocity can be phase-encoded by means of bipolar gradient pulses (or equivalently pairs of uni-polar gradient pulses separated by 180° refocusing pulses). It is thus clear that the insertion of bipolar gradient pulses between the RF-pulse elements will additionally sensitize these pulse trains to velocity. In this communication the principles of velocity selective perturbation will be described, and schemes for producing velocity selective excitation, saturation, and inversion presented, as will a simple method of combining velocity with slice selection.

[1] To whom correspondence should be addressed. Fax: ++49 341 99 40 221; e-mail: norris@cns.mpg.de.

THEORY

The simplest pulse train of this type is $1\ \bar{1}$ (90°–$\overline{90}$°), often known as "Jump and Return," was described in (*1*). It was subsequently found that the $1\ \bar{3}\ 3\ \bar{1}$ pulse with total angle 90° (*2, 7*) had superior properties for solvent suppression. Further refinements (*8–11*) brought pulses with improved excitation profiles albeit at the cost of increased length, complexity, and power deposition. The salient properties of RF-pulse trains as used in solvent suppression are:

(i) Perturbation is periodic along the frequency axis.

(ii) It is preferable to use pulse trains with an even number of RF-pulse elements, because the symmetry of the pulse train then means that errors in the pulse-gain setting cancel at the frequency of zero perturbation.

(iii) The effects of finite pulse duration are minimized by setting the RF carrier frequency to the solvent frequency.

(iv) With the notable exception of the "Jump and Return" pulse, the transverse magnetization generated by such pulse trains has a phase which is, to a good approximation, linearly dependent on the frequency offset.

These properties can largely be transferred directly to velocity selective perturbation. The effects of chemical shift and main field inhomogeneity can best be eliminated by inserting 180° refocusing pulses midway between RF-pulse elements. The velocity-encoding gradients are then placed about the refocusing pulse, as shown in Fig. 1. The total number of 180° pulses in the sequence should normally be kept even to ensure that non-selected magnetization is returned to the $+z$ axis at the end of the pulse train. If N, the total number of RF-pulse elements, is odd then only $N - 1$ refocusing pulses need be applied; for N even, each RF-pulse element should be followed by a refocusing pulse.

The gradient pulses induce a velocity-dependent phase change between each pair of RF-pulse elements given by

$$\phi = \gamma G v \delta \Delta, \qquad [1]$$

where G, δ, Δ are as defined in Fig. 1 and v is the velocity. At $v = v_{enc}$ the phase change induced between RF-pulse elements is π and in general the perturbation is maximal. This is a

1090-7807/99 $30.00

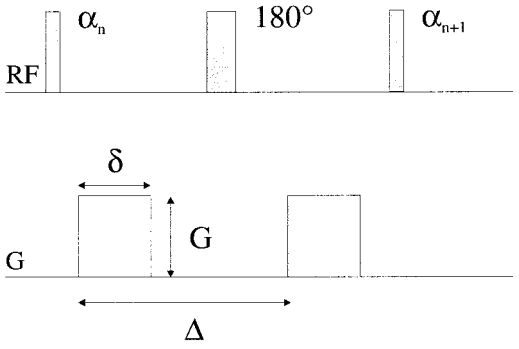

FIG. 1. Velocity-encoded perturbation. Only two RF-pulse elements of an excitation train are shown, separated by a 180° refocusing pulse midway between them. The velocity encoding is accomplished by means of the two gradient pulses, which in most situations will also be of sufficient strength to spoil transverse magnetization produced directly by the 180° pulse.

potential disadvantage of such schemes because this is also the velocity at which the direction of flow can no longer be distinguished. The first zero in the perturbation occurs at $v = 2v_{enc}$. Some of the more sophisticated pulse trains (*10, 8*) have unequal time intervals between RF-pulse elements. The velocity selective analogues require the velocity sensitization between RF-pulse elements to be proportional to the corresponding time interval in the original scheme. This may be achieved either by modifying the G, δ, or Δ either singly or in combination and hence the intervals between RF-pulse elements need not correspond to those in the original scheme. A fundamental difference between chemical shift and velocity selective perturbation is that the degree of velocity sensitization between RF-pulse elements may be varied by the experimenter, whereas the evolution of the chemical shift is determined by the inter-RF-pulse element duration alone.

Velocity selective pulse trains may be used to perturb either stationary or moving spins. In general RF-pulses are employed to fulfill one of four basic functions: saturation, excitation, inversion, and refocusing. These require efficient 90° and 180° pulses, which can also serve as the basis for obtaining other pulse angles if required. The specific requirements for velocity selective perturbation in these situations shall now be examined in turn.

Excitation and Saturation

Pulse trains for achieving 90° excitation have previously been developed and optimized (*10, 8*). In choosing a pulse train for a specific application the experimenter must consider the duration and power deposition against the efficiency of the pulse train. Following previous workers (*8*) we define the excitation/saturation efficiency, ψ_{es}, as the fraction of the period for which $M_{xy} > 0.9M_0$ or $M_z < 0.1M_0$, respectively, and note that a $1\ \bar{3}\ 3\ \bar{1}$ pulse has a ψ_{es} of 0.28 (*8*). As shown in Table 1 of Ref. (*8*), longer and more complex pulse trains can reach efficiencies of $\psi_{es} = 0.76$.

Especially in the case of saturation, considerably higher ψ_{es} values can be obtained by employing the concept of progressive velocity-encoded saturation which is proposed here. The pulse train illustrated in Fig. 1 is repeated m times. The strength of the bipolar gradients is linearly incremented by $\Delta G = G/m$ between successive blocks. Figure 2 shows the saturation profile calculated for a simple 90°–$\overline{90}$° train with $m = 6$. The corresponding saturation efficiency is $\psi_{es} = 0.88$.

Excitation requires the production of coherent transverse magnetization. As indicated above many chemical shift selective pulse trains produce a frequency dependent phase offset, and for most pulse trains this is approximately $180t$ degrees per Herz offset, where t is the pulse train duration in seconds (*8*). For velocity selective excitation this means that for a train with N RF-pulse elements the phase gradient is $N\pi$ per $2v_{enc}$. In contrast to a phase gradient produced by a chemical shift selective pulse train this phase gradient can be reversed by the application of an appropriate velocity sensitizing gradient pulse pair after the last RF-pulse element in the train. In direct analogy to the refocusing of slice selective excitation (*12*) the velocity sensitization of the refocusing gradient pulse pair is

$$\frac{-(N-1)\gamma G v \delta \Delta}{2},$$

where the velocity sensitization for each interval between RF-pulse elements is given by Eq. [1]. Either a bipolar gradient pulse or two unipolar pulses separated by a 180° refocusing pulse may be used. For rephasing, the sense of the velocity sensitization must of course be opposite to that used during the RF-pulse train.

Refocusing and Inversion

In many potential applications there is little practical difference in a spin-echo experiment between making either the 90° or the 180° pulse velocity selective. The RF-pulse trains pre-

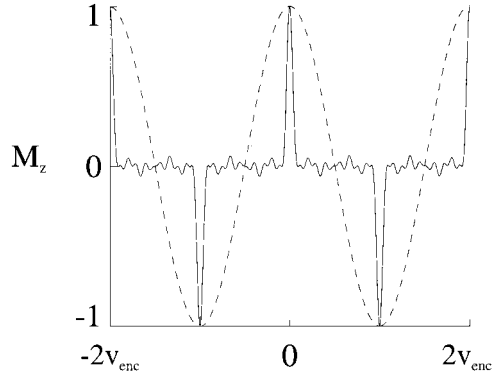

FIG. 2. Calculated saturation profile for the progressive velocity-encoded saturation sequence using a 90°–$\overline{90}$° train with $m = 6$ (solid line). The longitudinal magnetization is plotted against the velocity. For comparison the saturation profile produced by a single 90°–$\overline{90}$° train is shown (dashed line).

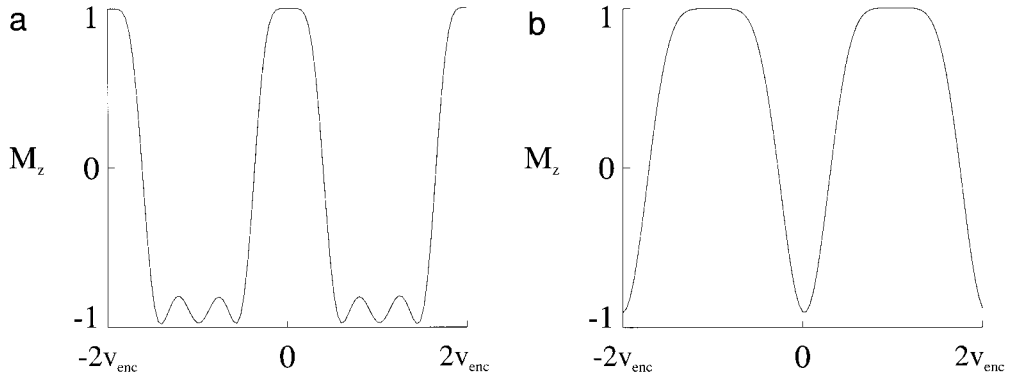

FIG. 3. Velocity selective inversion profiles obtained by computer simulation of the Bloch equations. (a) The longitudinal magnetization plotted against velocity for the $\overline{17.8}$–τ–$\overline{1.2}$–τ–32.9–τ–113.0–τ–$\bar{1}$ $\bar{1}$ $\bar{3}\tau$–$\overline{32.9}$–τ–1.2–τ–17.8 pulse train, which selectively inverts flowing spins. (b) The inversion profile for the 18.8–τ–58.9–τ–58.9–τ–18.8 pulse train.

sented here for inversion could also be used for spin refocusing, but experiments involving velocity selective refocusing shall not be further considered.

The use of RF-pulse trains to achieve solvent suppression generally requires a 90° excitation of the frequency range of interest. The simple attempt to use known excitation pulse trains to obtain a broad inversion of flowing spins will mostly be unsuccessful due to the nonlinearity of the Bloch equations. For example, if we define the inversion efficiency ψ_{in90} as the fraction of the period for which the longitudinal magnetization has a value of less than $-0.9M_0$ then a 2662 pulse (a 1331 pulse with a total angle of 180°) achieves a value of ψ_{in90} of 0.08. If velocity selective inversion is to be of value in practice then more efficient pulse trains are clearly required and these were sought by means of a computer simulation. In doing this it was also possible to consider the differing requirements for the inversion of flowing spins, which should normally occur over as broad a range of velocities as possible, and for stationary spins, which should be inverted, while flowing spins are left unperturbed. The method adopted closely followed that of Hall and Hore (*8*). Owing to the expected difficulty in finding good inversion pulse trains their quality was evaluated according to the value of ψ_{in80} rather than the more stringent ψ_{in90}. Pulse trains of the form

$$\alpha_1\text{–}n_1\tau\text{–}\alpha_2\text{–}n_2\tau\text{–}$$

were assessed. For inversion at non-zero velocity, pulse trains with both odd and even numbers of RF-pulse elements were considered, under the constraint that the first derivative of the rotation propagator at zero velocity be zero (*7*). Pulse trains with an even number of elements must then satisfy the condition that

$$\sum_{k=1}^{N-1} \sin \beta_k = 0, \qquad [2]$$

where

$$\beta_k = \alpha_1 + \alpha_2 + \cdots + \alpha_k. \qquad [3]$$

The solution of Eq. [2] was simplified by constraining all β_k apart from $\beta_{N/2}$ to have a modulus of less than 30° and hence allowing the coarse approximation $\sin \theta \approx \theta$. The program examined each permissible combination of α_k in steps of 1° for total pulse angles greater than 150°. ψ_{in80} was calculated for each pulse train and for each combination of n-values examined the best value of ψ_{in80} was noted. Promising pulse trains found in this way were re-examined by incrementing α_k by 0.1° within ±4° of the original value. The best pulse train found was

$$\overline{17.8}\text{–}\tau\text{–}\overline{1.2}\text{–}\tau\text{–}32.9\text{–}\tau\text{–}113.0\text{–}\tau\text{–}\bar{1}\ \bar{1}\ \bar{3}\text{–}\tau\text{–}\overline{32.9}\text{–}\tau\text{–}1.2\text{–}\tau\text{–}17.8$$

with $\psi_{in80} = 0.49$, and a total angle of 329.8°. The corresponding inversion profile is shown in Fig. 3a. For inversion at zero velocity, four-element pulse trains close to 2662 were examined. The criterion set here was that ψ_{in90}^{-}, defined as the fractional bandwidth for which $M_z > 0.9M_0$, be maximized. The aim of course was to achieve an inversion at zero velocity, and minimal perturbation at other velocities. The pulse train found was

$$18.8\text{–}\tau\text{–}58.9\text{–}\tau\text{–}58.9\text{–}\tau\text{–}18.8$$

with $\psi_{in90}^{-} = 0.41$, and $\psi_{in80}^{-} = 0.49$, and a total excitation angle of 155.4°. The inversion profile is shown in Fig. 3b. It should be emphasized that no assertion is made here that these pulse trains represent a global optimum: the aim is merely to find those with sufficiently good characteristics that the practical implementation can be demonstrated. No pulse trains

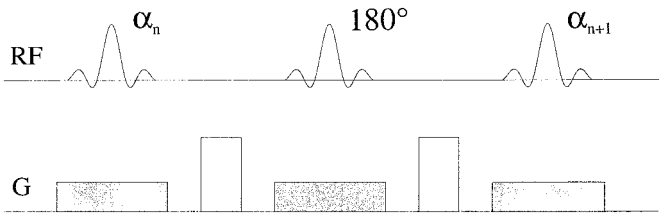

FIG. 4. Slice and velocity selective perturbation. As in Fig. 1 only two RF-pulse elements are shown. The shaded gradients are slice selective. The gradient strengths are not drawn to scale. It should be noted that the velocity-encoding gradients need not be parallel to those for slice encoding.

were found for inverting flowing spins which had a ψ_{in80} of greater than 0.4 and fewer than eight RF-pulse elements. For the inversion of non-flowing spins the search was not pursued beyond the simple form given above, because the properties were already as good as those of the inversion pulse train for flowing spins, which took considerably more effort to find.

In some situations a combination of slice and velocity selective perturbation would be desirable. Ideally this would occur simultaneously, as is the case for some spatial–spectral 2D pulses (*13, 14*). Although such pulses are theoretically possible, a simpler approach is proposed here, based on the separation of the slice and velocity selective functions in a fashion similar to that recently proposed for slice and chemical shift selective excitation (*15*). An example of a slice selective inversion scheme is shown in Fig. 4. It should be noted that due to the presence of the refocusing pulse no slice–rephase gradients are required. This would also be the case for a saturation pulse. A coherent excitation scheme would require a conventional refocusing gradient after the final RF-pulse element.

EXPERIMENTAL

All experiments were performed using a Bruker 3 T, 100 cm Medspec system and a Magnex head-gradient insert which has a performance of 35 mT/m within 150 μs. Transmission and reception were performed using a standard circularly polarized birdcage resonator of 280 mm i.d. A constant-head flow phantom was used to generate laminar flow through plastic tubing of 19 mm i.d. The phantom used consisted of the outward and return sections of the tubing, plus two stationary bottles, doped with $NiCl_2$ to give T_1 values of approximately 500 and 1600 ms. In all the images shown the two bottles are above the tubing with the bottle having the T_1 value of 500 ms on the right. The proton densities of all parts of the phantom were roughly equal, and the difference in T_1 values between the two stationary bottles could be used to test the quality of inversion. The total flow rate in the phantom was 0.32 L/min, which under the justified assumption of laminar flow corresponds to a maximum velocity of 38 mm/s. The flow-encoding gradients used were of strength 7.35 mT/m, δ was 5.2 ms, and Δ was 8.7 ms, which, using the notation of Eq. [1], gives a flow sensitivity of 88.5 s rad/m; i.e., v_{enc} corresponded to the maximum velocity present. The $\mathbf{B}_1$ field strength in all the velocity-encoding RF-pulse trains was 36 μT, corresponding to a 180° inversion pulse duration for protons of 3.28 ms. In the majority of experiments it was sufficient to prepare the magnetization along the longitudinal axis, and here imaging was performed using a snapshot-FLASH experiment (*16*) with the following parameters: FOV, 120 mm; slice thickness, 5 mm; *TE*, 2.2 ms, *TR*, 4.35 ms, flip angle, 15°; Gaussian pulse form, acquisition bandwidth 80 kHz; data matrix, 128 (read) by 64. In the velocity selective excitation experiments, which require coherent transverse magnetization a spin-echo experiment was employed in which the refocusing pulse was a slice selective 180° (*17*). The velocity refocusing was performed by inserting the appropriate bipolar gradient pulses after the 180° pulse. The geometric parameters were the same in both experiments, and other experimental parameters were: *TE*, 39 ms; *TR*, 1 s. In the slice and velocity selective inversion, sinc pulse elements of 2 ms duration were employed. The slice inverted was 1.5 times broader than the FWHM of the Gaussian excitation pulse in the subsequent snapshot-FLASH experiment.

The results obtained for saturation and excitation are presented in Fig. 5. In (a) and (b) the saturation of non-flowing and flowing material is depicted; in (c) and (d) the corresponding excitation images are shown. A simple 121 or $1\bar{2}1$ RF-pulse train was used as appropriate. The effects of the laminar flow profile are visible in all these images. Figure 6 shows the results of control inversion–recovery measurements without

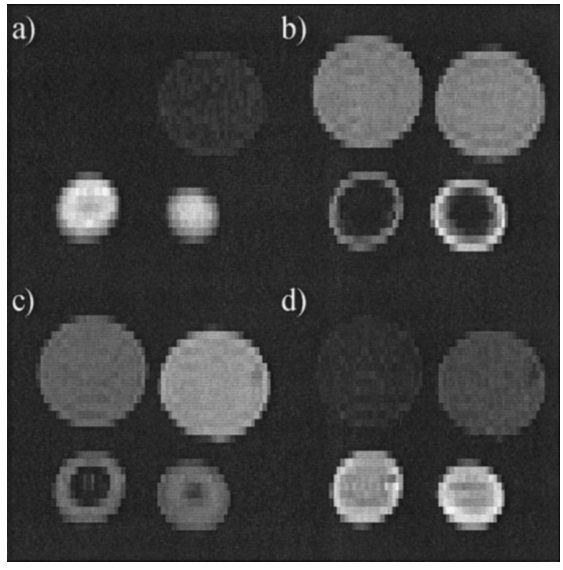

FIG. 5. Velocity selective saturation and excitation. In each image a 121 type pulse train was used for velocity encoding. (a) The saturation of stationary spins. (b) The saturation of flowing spins. (c, d) The same experiments with excitation used instead of saturation. In (a) and (b), imaging was performed using a snapshot-FLASH experiment; in (c) and (d), a spin-echo sequence was used. Despite the different imaging sequences used the correspondence between the images is good in that saturation produces images that are the inverse of those produced by excitation.

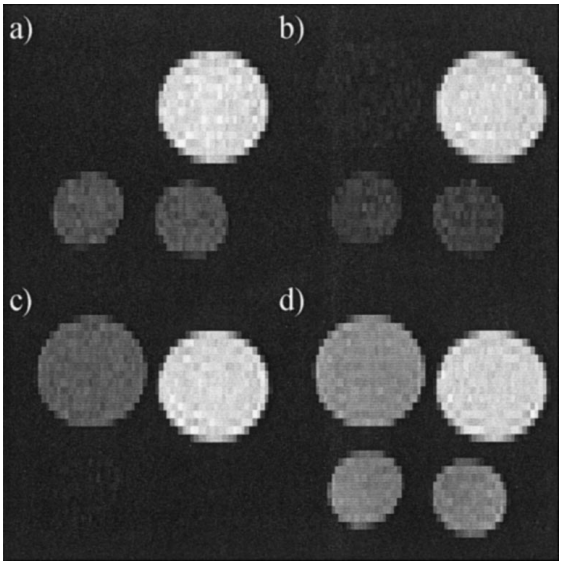

FIG. 6. Control inversion–recovery experiments in the absence of flow. (a) Inversion using a standard hyperbolic secant pulse. (b) The velocity selective inversion of stationary spins using the $18.8-\tau-58.9-\tau-58.9-\tau-18.8$ pulse train. (c) Use of the slice selective version. (d) Testing of the $\overline{17.8}-\tau-\overline{1.2}-\tau-32.9-\tau-113.0-\tau-\bar{1}\ 1\ \bar{3}-\tau-\overline{32.9}-\tau-1.2-\tau-17.8$ pulse train for the inversion of flowing material.

flow. In all images the inversion time was 1 s, which results in a low signal intensity for all but the right bottle, the left bottle being close to the zero transition. The hyperbolic secant (sech) pulse is known to provide high quality inversion over a wide range of $\mathbf{B}_1$ values, and hence a lower quality of inversion for the velocity selective pulse trains should give rise to noticeable changes in signal intensity for the left bottle. In (a), a sech inversion pulse of 10 ms was applied, in (b) the result from the inversion of non-flowing material is shown, and in (c) the combination of slice and velocity selective inversion is shown. In (b) and (c) the optimized RF-pulse train for inversion of non-flowing material described above was used. The inversion is qualitatively somewhat worse in 6b than in 6a and deteriorates further when slice selection is incorporated. Figure 6d shows the control inversion of flowing spins, again using the optimized RF-pulse train for this purpose described above. It is clear that the magnetization of the stationary spins is perturbed to a limited extent by this pulse train as otherwise all the objects shown in Fig. 6d would show the same intensity. Finally, Fig. 7 shows the inversion experiments with flow. Figure 7a results from the inversion of stationary material. As expected, the non-inverted flowing spins give the maximum signal intensity. The slice selective variant is shown in (b). The high intensity of the signal in the tubes is caused by inflow during the 1 s inversion delay. As expected, the inversion of flowing spins in (c) results in the near nulling of the signal in the center of the tubes.

DISCUSSION AND CONCLUSIONS

In this communication the principles of velocity selective perturbation have been demonstrated for the standard applications of RF-pulses. Both simple and complex pulse trains have been shown in practice to perform broadly as expected. The major advantage of these pulse schemes is that moving spins can be directly magnetically labeled on the basis of their velocity and independently of position.

The differing types of pulse train presented vary considerably in terms of their utility. The potential for velocity selective excitation is probably somewhat limited. Refocusing the phase distribution produces coherently excited spins, but in biomedical applications it is to be expected that these rapidly dephase under the influence of static magnetic field gradients. Saturation has a number of advantages: as shown above, progressive velocity-encoded saturation yields an excellent saturation profile, and rapid sequential saturation with the velocity-encoding gradients applied successively in three orthogonal directions makes the experiment independent of the direction of flow. These considerations apply self-evidently to the saturation of flowing spins: the saturation of stationary material inevitably includes that moving perpendicular to the gradient direction. An alternative approach is to use the successive inversion of moving spins with the sensitizing gradients applied in three orthogonal directions to make the experiment independent of the direction of motion.

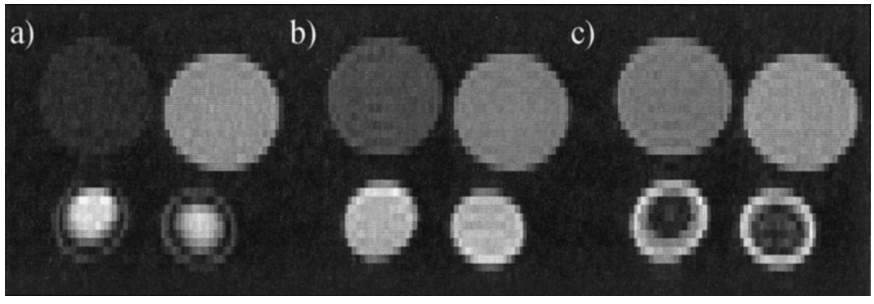

FIG. 7. Velocity selective inversion–recovery experiments. The water in the tubes is flowing; otherwise the experimental parameters shown in (a), (b), and (c) are the same as those for Figs. 6b, c, and d, respectively. The high signal intensity in the tubes in (b) is caused by inflow during the inversion time rather than any improvement in the inversion profile compared to (a).

Technical limitations of the pulse schemes demonstrated here are that, dependent on the characteristics of the gradient system used, they are of relatively lengthy duration, and the requirement to insert a refocusing pulse between RF-pulse elements means that, particularly the more complex schemes have a high power deposition. It is unlikely that such schemes could be implemented on systems without good self-shielded gradient coils.

Conceivable applications for these pulse trains can be found in the fields of flow and angiography, motion and in-flow desensitization, and perfusion. As shown above it is possible to directly image spins within a defined range of velocities. However, the main potential benefit in angiography is that the presaturation of stationary spins should mean that flowing material is imaged under ideal conditions. Instead of saturating spins within a slice or slab and waiting for inflow to occur all flowing spins should yield a signal intensity that is independent of position. The pre-saturation of moving spins should reduce in-flow and motion artefacts without the complications imposed by the slice selective saturation of neighboring slices. Similarly, in functional imaging inflow effects could be reduced, and saturation of the venous compartment could improve the localization of activation to the parenchyma.

In recent years significant progress in perfusion imaging has been made using spin labeling methods (*18–21*). Velocity selective perturbation could improve these methods by labeling blood closer to the imaging plane without significantly perturbing slow moving or stationary spins. As the blood flow is greater in the arteries the gradient requirements are significantly reduced by labeling it here. Perfusion measurement usually relies on taking the difference between a perfusion sensitized and a non-sensitive control image with otherwise identical contrast. Such control images could be obtained by removing the flow-sensitizing gradients, or by nulling their first moment. Cross-talk due to the flow of labeled blood between slices could be eliminated by the use of such pulse trains, making them eminently applicable to multislice perfusion imaging.

ACKNOWLEDGMENT

The authors thank Manfred Weder for technical assistance.

REFERENCES

1. P. Plateau, C. Dumas, and M. Gueron, Solvent-peak-suppressed NMR: Correction of baseline distortions and use of strong-pulse excitation, *J. Magn. Reson.* **54,** 46–53 (1983).
2. P. J. Hore, A new method for water suppression in the proton NMR spectra of aqueous solutions, *J. Magn. Reson.* **54,** 539–542 (1983).
3. M. Gueron, P. Plateau, and M. Decorps, Solvent signal suppression in NMR, *JPNMRS* **23,** 135–209 (1991).
4. E. L. Hahn, Detection of sea-water motion by nuclear precession, *J. Geophys. Res.* **65,** 776–777 (1960).
5. P. R. Moran, A flow velocity zeugmatographic interlace for NMR imaging in humans, *Magn. Reson. Imag.* **1,** 197–203 (1983).
6. T. W. Redpath, D. G. Norris, R. A. Jones, and J. M. S. Hutchison, A new method of NMR flow imaging, *Phys. Med. Biol.* **29,** 891–898 (1984).
7. P. J. Hore, Solvent suppression in Fourier transform nuclear magnetic resonance, *J. Magn. Reson.* **55,** 283–300 (1983).
8. M. P. Hall, and P. J. Hore, Computer-optimized solvent suppression, *J. Magn. Reson.* **70,** 350–354 (1986).
9. Z. Starcuk and V. Sklenar, New hard pulse sequences for the solvent signal suppression in Fourier-transform NMR, I, *J. Magn. Reson.* **61,** 567–570 (1985).
10. Z. Starcuk and V. Sklenar, New hard pulse sequences for the solvent signal suppression in Fourier transform NMR, II, *J. Magn. Reson.* **66,** 391–397 (1986).
11. G. A. Morris, K. I. Smith, and J. C. Waterton, Pulse sequences for solvent suppression with minimal spectral distortion, *J. Magn. Reson.* **68,** 526–532 (1986).
12. R. J. Sutherland and J. M. S. Hutchison, Three-dimensional NMR imaging using selective excitation, *J. Phys. E: Sci. Instrum.* **11,** 79–83 (1978).
13. J. Pauly, D. Nishimura, and A. Macovski, A k-space analysis of small-tip-angle excitation, *J. Magn. Reson.* **81,** 43–56 (1989).
14. J. Pauly, D. Nishimura, and A. Macovski, A linear class of large-tip-angle selective excitation pulses, *J. Magn. Reson.* **82,** 571–587 (1989).
15. F. Schick, J. Forster, J. Machann, P. Huppert, and C. D. Claussen, Highly selective water and fat imaging applying multislice sequences without sensitivity to B1 field inhomogeneities, *Magn. Reson. Med.* **38,** 269–274 (1997).
16. A. Haase, Snapshot FLASH MRI. Applications to T1, T2, and chemical-shift imaging, *Magn. Reson. Med.* **13,** 77–89 (1990).
17. J. Mao, T. H. Mareci, and E. R. Andrew, Experimental study of optimal selective 180 radiofrequency pulses, *J. Magn. Reson.* **79,** 1–10 (1988).
18. D. S. Williams, J. A. Detre, J. S. Leigh, and A. P. Koretsky, Magnetic resonance imaging of perfusion using spin inversion of arterial water, *Proc. Natl. Acad. Sci. U.S.A.* **89,** 212–216 (1992).
19. J. A. Detre, J. S. Leigh, D. S. Williams, and A. P. Koretzky, Perfusion imaging, *Magn. Reson. Med.* **23,** 37–45 (1992).
20. R. R. Edelman, B. Siewert, D. G. Darby, V. Thangaraj, A. C. Nobre, M. M. Mesulam, and S. Warach, Qualitative mapping of cerebral blood flow and functional localization with echo-planar MR imaging and signal targeting with alternating radio frequency, *Radiology* **192,** 513–520 (1994).
21. K. K. Kwong, D. A. Chesler, R. M. Weisskoff, K. M. Donahue, T. L. Davis, L. Ostergaard, T. A. Campbell, and B. R. Rosen, MR perfusion studies with T1-weighted echo planar imaging, *Magn. Reson. Med.* **34,** 878–887 (1995).